Regarding the Effect that Different Hydrocarbon/Fluorocarbon Surfactant Mixtures Have on Their Complexation with HSA

Elena Blanco,[†] Paula Messina,[‡] Juan M. Ruso,*,[†] Gerardo Prieto,[†] and Félix Sarmiento[†]

Group of Biophysics and Interfaces, Department of Applied Physics, Faculty of Physics, University of Santiago de Compostela, E-15782 Santiago de Compostela, Spain, and Grupo de Ciencia de Superficies y Coloides, Departamento de Química, Universidad Nacional del Sur, 8000 Bahía Blanca, Argentina

The complexations between human serum albumin (HSA) and the sodium perfluorooctanoate/sodium octanoate and sodium perfluorooctanoate/sodium dodecanoate systems have been studied by a combination of electrical conductivity, ion-selective electrode, electrophoresis, and spectroscopy measurements. The binary mixtures of the surfactants deviated slightly from ideality. Binding plots revealed the existence of two specific binding sites, the first site being more accessible than the second. Positive cooperative binding has been found, thus revealing the importance of the hydrophobic interactions in both kinds of surfactants. The Gibbs energies of binding per mole of surfactant ($\Delta G_{\bar{\nu}}$) were calculated from the Wyman binding potential where, on the basis of the elevated number of binding sites, a statistical contribution has been included. Initially these energies are large and negative, gradually decreasing as saturation is approached. Changes in the slope of Gibbs energies have been identified with the saturation of the first binding set. These facts denote that the surfactants under study have different favorite adsorption sites along the protein and that the adsorption process of perfluorooctanoate is more closely followed by dodecanoate than by octanoate. Finally, electrophoresis and spectroscopy measurements suggest induced conformational changes on HSA depending on the surfactant mixture as well as the mixed ratio.

1. Introduction

Early works addressed the interactions of small molecules with proteins because of their biological function. These interactions result, for example, in folding and binding, two of the most fundamental aspects of protein behavior. Over the last several decades, these have been used in several biotechnological disciplines (control of colloidal stability in foods and pharmaceuticals, construction of nanodevices, etc.[1]). Moreover, mixtures of proteins and surfactants occur in response to several different thermodynamic driving forces, and as a result the mode of binding and the supramolecular structure of the resulting complexes are quite sensitive to solution composition and temperature, which is interesting from a theoretical standpoint.[2] However, there are relatively few articles that deal with the interactions of proteins with surfactant mixtures.

Research on surfactant mixtures is of considerable interest for numerous technical applications because surfactant mixtures enhance performance when compared to single surfactants. On the other hand, because of hydrophobicity between fluorocarbons and hydrocarbons, mixed fluorocarbon and hydrocarbon surfactants exhibit nonideality when it comes to the mixing of their micelles. The important characteristic of the immiscibility of two surfactants is the coexistence of two kinds of monolayers featuring different compositions.[3] In many cases, the combination of fluorocarbon surfactant plus a suitable hydrocarbon surfactant can produce a degree of wetting which cannot be attained by either type alone. In such a combination, it is typically the fluorocarbon surfactant which reduces the surface tension (air−water surface), whereas the hydrocarbon surfactant aids in the reduction of the interfacial tension (oil−water surface). The net result can be a system that easily wets and spreads on otherwise hard to wet surfaces. However, fluorocarbon surfactants are generally expensive and, in many applications, a combination of fluorocarbon and hydrocarbon surfactants is economically preferable.[4]

We have recently focused our research on the interactions between proteins and hydrocarbon and fluorocarbon surfactants with a view to understanding the mechanism responsible for the adsorption of these molecules to such biopolymers,[5−7] and on the study and comparison of the physicochemical properties of hydrogenated surfactants and their corresponding perfluorinated ones as a function of temperature and alkyl chain.[8] Hence, our aim in this article is to build upon the knowledge in this area in several ways. On one hand, we are trying to clarify the interaction of proteins with surfactant mixtures and, on the other hand, we are trying to enhance the physicochemical properties of hydrocarbon/fluorocarbon surfactant mixtures in the presence of biopolymers. For this purpose, we have chosen human serum albumin, sodium perfluorooctanoate, sodium octanoate, and sodium dodecanoate.

The globular protein human serum albumin (HSA), consisting of 583 amino acids in a single polypeptide chain with a molar mass of 66 500 g mol^{-1}, is widely used as a model protein in the study of such interactions.[9] X-ray crystallography[10] has shown an asymmetric heart-shaped molecule with sides of 8 nm and thickness of 3 nm that can be roughly described as an equilateral triangle with a height of 6.9 nm. The two heart lobes contain the molecule's hydrophobic binding sites while the outside of the molecule contains most of the polar groups. HSA constitutes approximately half of the total blood protein, acting

* To whom correspondence should be addressed. E-mail: faruso@usc.es.
† Group of Biophysics and Interfaces.
‡ Grupo de Ciencia de Superficies y Coloides.

as a carrier for fatty acids and several amphiphiles from bloodstream to tissues, and hence is an appropriate choice of protein for use in a study of interaction with amphiphilic compounds.

Sodium perfluorooctanoate, sodium octanoate, and sodium dodecanoate have been chosen because their solution properties have been widely characterized in previous works and because these surfactants allow us to compare the differences between hydrocarbon/fluorocarbon mixtures with the same alkyl chain with mixtures where the hydrocarbon chain is 1.5 times longer than the fluorocarbon chain (it is well-known that in this relation both surfactants have the same critical micellar concentration[11]).

This paper is organized as follows. Initially we studied the properties of both surfactant mixtures trying to determine the existence of synergism, the critical micellar concentration, and the interaction parameters. We then introduced the HSA, explaining the different complexation pattern on the basis of their mixture properties.

2. Experimental Section

2.1. Materials. Sodium octanoate (C8HONa) and sodium perfluorooctanoate (C8FONa) of at least 97% purity were obtained from Lancaster Synthesis Ltd. Sodium dodecanoate (C12HONa) with purity greater than 99% was obtained from Sigma Chemical Co. Human serum albumin (HSA, albumin ($\geq$96%), essentially fatty acid free, product no. A-1887) was purchased from Sigma Chemical Co. with a molecular weight of 66 500 Da and containing 585 amino acid residues. All of these products were used as received. All measurements were performed using distilled water with conductivity below 3 μS cm^{-1} at 298.15 K. Protein concentration (0.125 mg/mL) was kept constant in all experiments. The measurements were performed at 298.15 $\pm$ 0.01 K throughout all the experiments.

2.2. Electrical Conductivity. Conductance was measured by using a conductivity meter (Kyoto Electronics type C-117), the cell of which (Kyoto, type K-121) was calibrated with KCl solutions in the appropriate concentration range. The cell constant was calculated using molar conductivity data published by Shedlovsky[12] and Chambers et al.[13] The measuring cell was immersed in a Polyscience PS9105 thermostated bath, maintaining the temperature constant to within $\pm$0.01 K.

2.3. Electrophoresis. Electrophoretic mobility measurements were taken using a Malvern Instruments Ltd Zetamaster 5002. The cell used was a 5 mm $\times$ 2 mm rectangular quartz capillary. The mobilities were taken as the average of at least 10 measurements, at stationary level, considering their standard deviation as the experimental error. The zeta potentials were calculated from the electrophoretic mobility by means of the Henry correction of Smoluchowski's equation.[14]

2.4. Spectroscopy. Difference spectra were measured using a Beckman spectrophotometer (model DU 640), with six microcuvettes, operating in the UV$-$visible region, with a full scale expansion of 0.2 absorbance units. For absorbance difference spectra, five of the six microcuvettes were filled with protein plus surfactant solutions. The first microcuvette contained only protein in the corresponding medium and was used as a blank reference. The microcuvettes were filled and placed in the same position for all the tests. Absorbance was measured at a temperature of 298.15 $\pm$ 0.01 K using a temperature controller (Beckman DU Series), based on the Peltier effect.

2.5. Ion-Selective Electrode. Potentiometric determinations were made with a millivoltmeter and a CRISON pH meter. The millivoltmeter was used with C8FO$^-$, C8HO$^-$, and C12H$^-$ ion-selective electrodes against a saturated calomel electrode.

The ion-selective electrode was made by gluing at one end of a poly(vinyl chloride) (PVC) tube, a membrane made with 300 mg of PVC dissolved in 50 mL of tetrahydrofuran (THF), 0.2 mL of dibutylphthalate (plasticizer), and 0.167 g of an insoluble ion salt. The insoluble salt was filtered and washed several times with double-distilled water and then left to dry. The crystals were powdered and suspended in the PVC solution. The suspension was then left in a Petri dish to let the THF evaporate, and the resulting membrane was cut and glued to the tube. The tube was filled with an internal solution. An Ag/AgCl electrode made with a silver wire was placed into the tube and connected to the millivoltmeter by a copper wire passing through a rubber plug.

The scheme of the electrode is as follows: Ag/AgCl// reference solution/PVC membrane/sample//AgCl/Ag. The time response of the electrode depends on solution concentrations, added electrolyte, stirring, and conditioning. In dilute solutions, the time required to get stable emf values was 2 min.

The ion-selective electrodes are sensitive to the respective free (nonaggregated) ion activity. Working with a diluted ion solution without protein below critical micelle concentration (cmc) and assuming that all surfactant present in the solution is free and that activities depend on concentrations, we made an emf versus free ion concentration calibration curve. This calibration curve was employed to obtain the free ion concentration for the HSA$-$surfactants interaction.

C8FO$^-$ Ion Selective Electrode. Insoluble Salt of the Electrode Membrane. The insoluble Ba^{2+}(C8FO$^-$)$_2$ salt was made by mixing the appropriate amounts of Ba(OH)$_2$ and C8FO$^-$ Na$^+$ aqueous solution.

Internal Solution. The internal solution was made by mixing equals parts of aqueous solution of 0.01 mol dm^{-3} C8FO$^-$ Na$^+$ and 0.1 mol·dm^{-3} KCl containing a small amount of solid AgCl.

C8HO$^-$ Ion Selective Electrode. Insoluble Salt of the Electrode Membrane. The insoluble La^{3+}(C8HO$^-$)$_3$ salt was made by mixing the appropriate amounts of La^{3+}(NO$_3$$^-$)$_3$ and C8HO$^-$ Na$^+$ aqueous solution.

Internal Solution. The internal solution was made by mixing equals parts of aqueous solution of 0.01 mol dm^{-3} C8HO$^-$ Na$^+$ and 0.1 mol·dm^{-3} KCl containing a small amount of solid AgCl.

C12HO$^-$ Ion Selective Electrode. Insoluble Salt of the Electrode Membrane. The insoluble La^{3+}(C12HO$^-$)$_3$ salt was made by mixing the appropriate amounts of La^{3+}(NO$_3$$^-$)$_3$ and C12HO$^-$ Na$^+$ aqueous solution.

Internal Solution. The internal solution was made by mixing equals parts of aqueous solution of 0.01 mol dm^{-3} C12HO$^-$ Na$^+$ and 0.1 mol dm^{-3} KCl containing a small amount of solid AgCl.

3. Results and Discussion

Aqueous solutions of the C8HONa/C8FONa and C12HONa/C8FONa systems have been characterized through electrical conductivity measurements. For the first system, two breaks were observed for all mixed ratios, whose values are the same as those corresponding to the pure surfactants, suggesting the absence of mixing. A similar conclusion was previously reached for mixtures of fluorocarbon and hydrocarbon surfactants with short chain surfactants.[15] The critical micellar concentrations (cmc$_m$) for the C12HONa/C8FONa system are plotted in Figure 1 as a function of the mixed ratio, α_F (subscripts F, H, and m correspond to C8FONa, C12HONa, and mixture, respectively). In previous studies for this system, discrepancies have arisen for cmc$_m$ values in the C12HONa rich region;[16,17] however, in the present case our values corroborate those reported by De
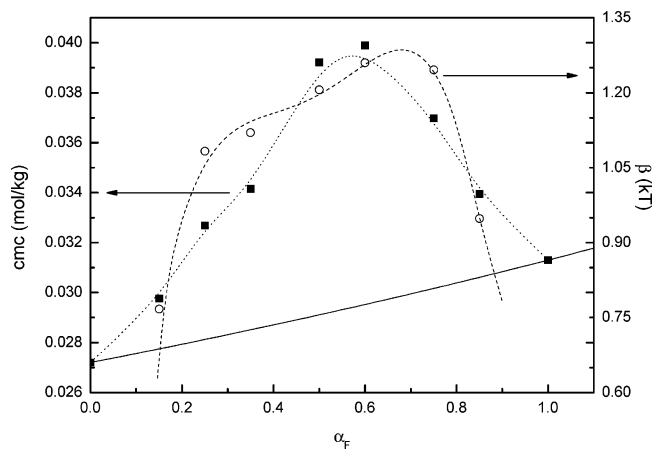
Figure 1. (■) Dependence of the critical micelle concentrations (cmc$_m$) of the C12HONa/C8FONa system as a function of α_1. (○) Interaction parameter in mixed micelles as a function of α_1. The solid line corresponds to the theoretical cmc$_m$ values predicted by the RST.

Lisi et al.[16] The cmc$_m$ values predicted by the regular solution theory[18] (RST) have been plotted in Figure 1 (solid line), and it can be observed how cmc$_m$ experimental values deviate positively from the ideal ones. β is the dimensionless RST interaction parameter, which is related to the molecular interactions in the mixed micelles. The value of β for the interactions in a mixed micelle can be calculated from the equations[19]

$$\frac{X_1^2 \ln(\alpha_1 cmc_m/(X_1 cmc_1))}{(1 - X_1)^2 \ln[(1 - \alpha_1)cmc_m/((1 - X_1)cmc_2)]} = 1 \quad (1)$$

$$\beta = \frac{\ln(\alpha_1 cmc_m/(X_1 cmc_1))}{(1 - X_1)^2} \quad (2)$$

where X_1 and X_2, are the mixed micelle composition in equilibrium with solution monomers of composition α_1 and α_2 (the mole fractions on a surfactant-only basis, so that $X_1 + X_2 = 1$ and $\alpha_1 + \alpha_2 = 1$). Equation 1 is solved for X_1, which is then replaced in eq 2 to obtain β. Hoffmann and Pössnecker[20] have demonstrated by error expansion of eq 1 that the minimum error for β in a single determination is nearly 0.1 $k_B T$ (k_B being the Boltzmann constant and T the absolute temperature). The error value rises quickly when one component in the micelle dominates. Values obtained for β (in $k_B T$ units) as a function of α_1 have been plotted in Figure 1.

β indicates the nature and strength of the interaction between two surfactants. In other words, it is a measure of the degree of nonideality in mixed micelles: the larger the negative value of β is, the stronger the attractive interaction between the two different surfactant molecules is, and the greater the synergism between them is. Meanwhile, positive values yield repulsive interactions (naturally $\beta = 0$ indicates an ideal mixture). Positive β values have been found for our system which is common in mixtures of fluorocarbon−hydrocarbon surfactants.[21] Typical values of β are +2.2 for lithium dodecyl sulfate−lithium perfluorooctanesulfonate.[22] As is the case in several systems, β was not constant and reflects the changes in the interaction energy when the micelle composition changes. These results indicate that there is a repulsion of fluorocarbon against hydrocarbon.

The potentiometric data have allowed for the construction of the binding isotherms. Figures 2 and 3 show the binding isotherms for the C8HONa/C8FONa and C12HONa/C8FONa systems on human serum albumin plotted as the number of
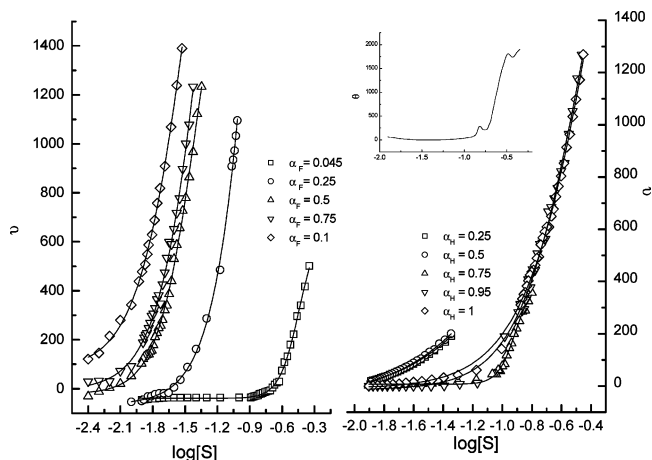

Figure 2. Binding isotherms (number of adsorbed surfactant molecules for protein molecule) of sodium perfluorooctanoate (left-hand plots) and sodium octanoate (right-hand plots) to human serum albumin at different mixed ratios (α) as a function of the logarithm of the total concentration. The solid lines correspond to the best fits to eq 4. The inset shows an example of the binding capacity.
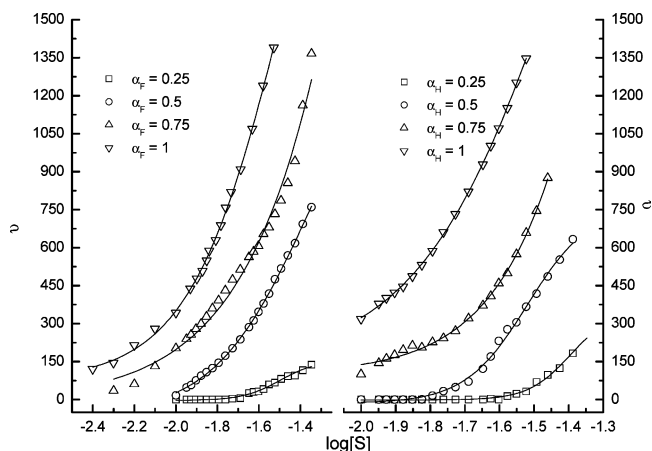

Figure 3. Binding isotherms of sodium perfluorooctanoate (left-hand plots) and sodium dodecanoate (right-hand plots) to human serum albumin at different mixed ratios (α) as a function of the logarithm of the total concentration. The solid lines correspond to the best fits to eq 4.

surfactant molecules per protein molecule, $\bar{\nu}$, as a function of the logarithm of the total concentration. All of the isotherms are for the free surfactant concentrations below the cmc$_m$ values. As could be expected, these plots are characteristic for interaction between amphiphilic molecules and globular proteins: a noncooperative binding region at low surfactant concentrations and a cooperative binding at the higher ones. However, some general features can be observed. First of all, the composition of the monomer in solution (both α_F and α_H) is increased, the noncooperative region decreases for the C12HONa/C8FONa system, while in the case of the C8HONa/C8FONa system, the noncooperative region increases for α_H. These facts are intimately related with the ability to form mixed micelles studied at the beginning of this section. On the other hand, the number of molecules adsorbed onto the protein is higher for C8FONa than for C8HONa, because of the higher hydrophobicity of the former, but it is similar for C8FONa and C12HONa. In a previous work we demonstrated not only that the cmc of a perfluorinated surfactant is approximately equal to that of a hydrocarbon surfactant with a hydrocarbon chain 1.5 times longer, but also that the thermodynamic quantities of micellization and apparent volumes satisfy this ratio as well, which

are related by the relation 1.5. Thus, it is possible that this relation could be extended to the interaction with macromolecules. A final remark can be made on the basis of a comparison of the binding isotherms of C8FONa at lower α_F. The value is lower when C8FONa is mixed with C12HONa than with C8HONa; probably the higher length of the alkyl chain of the C12HONa when it is adsorbed onto the protein prevents C8FONa being absorbed onto the surrounding places. A similar conclusion has been reached for the interactions between cesium and tetraalkylammonium dodecyl sulfates and poly(ethylene oxide) or poly(vinylpyrrolidone); the larger the counterion radius is, the smaller the interaction is.[23]

The binding isotherms for these systems range up to $\bar{\nu}$ values of 1395, 1269, and 1350 for pure C8FONa, C8HONa, and C12HONa respectively, while at mixed ratios of 50% the average numbers found were 194/1231 for C8HONa/C8FONa, and 633/762 for C12HONa/C8FONa. Human serum albumin is composed of 585 amino acids,[24] so with these values we obtain an approximate value of 2 molecules per amino acid residue, thus suggesting a small clustering of surfactants along the polypeptide chain. Such a cluster size is far from the aggregation numbers of the corresponding micelles and which is typical for interactions between surfactants and polymers and proteins. However, these data do not enable us to draw any conclusions about the uniformity of binding along the polypeptide chain, although it is likely that binding is greater (and cluster size larger) around hydrophobic amino acid residues and in hydrophobic cavities in the protein and less around hydrophilic residues.

A powerful tool in obtaining greater knowledge about the binding isotherms is the binding capacity which is defined, considering the ideal behavior, by

$$\theta = \left(\frac{\partial \bar{\nu}}{\partial \mu_i}\right)_{T,P,\mu_{i\neq j}} = \left(\frac{\partial \bar{\nu}}{2.303RT\, \partial \log[S]}\right)_{T,P,\mu_{i\neq j}} \tag{3}$$

where R is the gas constant, T the absolute temperature, μ_i the chemical potential of the ligand i, and [S] the free surfactant concentration. This quantity represents the change in the number of moles of ligand per mole of macromolecule that accompanies a change in the chemical potential of that ligand and provides a measure of the steepness of the binding isotherm.[25] The binding capacity curve can easily be obtained from the slope of the curves represented in Figures 2 and 3. The binding capacity curve consists of a series of consecutive maxima, the number of which is equal to the number of binding sets. For our systems the number of maxima found was two, consequently the binding data were adapted to the Hill equation for two sets of binding sites:

$$\bar{\nu} = \left\{\frac{g_1(K_1[S])^{n_1}}{1 + (K_1[S])^{n_1}}\right\} + \left\{\frac{g_2(K_2[S])^{n_2}}{1 + (K_2[S])^{n_2}}\right\} \tag{4}$$

where g_1, K_1, n_1, and g_2, K_2, n_2, are the number of binding sites, the binding constant, and the Hill coefficient for the first and second binding sets, respectively. The results obtained from the fitting of experimental points to eq 4 are listed in Table 1. Two interesting conclusions can be extracted from these results. For all systems, K_1 is higher than K_2 and g_2 is higher than g_1. The first result indicates that initial binding is stronger while the second result, more binding sites in the second step, could indicate that the protein is unfolded, making the hydrophobic residues accessible to the surfactant molecules. Values for n_1 and n_2 are higher than 1, meaning that the binding is positively

TABLE 1: Parameter Obtained from Equation 4[a]

			C8HONa/C8FONa System			
α_F (C8FO$^-$) or α_H (C8HO$^-$)	g_1	K_1	n_1	g_2	K_2	n_2
			C8FO$^-$ Ion Selective Electrode			
0.042	500	1400	3.8	1524	1120	2.7
0.25	484	1382	2.8	1302	1280	2.2
0.5	658	1419	3.6	1268	1242	2.2
0.75	732	1444	2.4	2041	1211	2.1
1	753	1418	2.4	1926	1113	1.6
			C8HO$^-$ Ion Selective Electrode			
0.25	211	1250	2.2	1776	1127	1.6
0.5	359	1270	2.5	1553	1172	2.5
0.75	366	1382	3.1	1905	1231	2.9
0.94	409	1353	3.1	1390	1233	1.9
1	413	1328	2.1	2132	1264	2.9
			C12HONa/C8FONa System			
α_F (C8FO$^-$) or α_H (C8HO$^-$)	g_1	K_1	n_1	g_2	K_2	n_2
			C8FO$^-$ Ion Selective Electrode			
0.25	546	1065	6.3	1329	929	2.3
0.5	609	1146	5.0	1397	1140	3.4
0.75	699	1268	5.5	1565	1147	4.3
1	753	1418	2.4	1926	1113	1.6
			C12HO$^-$ Ion Selective Electrode			
0.25	580	1236	4.6	1289	1100	2.8
0.5	567	1312	4.8	1426	1178	3.2
0.75	684	1395	4.3	1538	1190	2.6
1	749	1408	4.4	2066	1204	2.4

[a] Estimated uncertainties: ±15% for K_1, K_2, g_2 and ±10% for g_1, n_1, and n_2.

cooperative, the binding of a ligand enhancing the binding of subsequent ligands, thus highlighting the importance of the hydrophobic interactions. Hill coefficients are higher for the C12HONa/C8FONa system where the existence of mixed micelles has already been revealed. A similar behavior has been found for interactions between cationic surfactants and bovine serum albumin.[26]

The Gibbs energies of binding per mole of surfactant ($\Delta G_{\bar{\nu}}$) were calculated from the Wyman binding potential (π) derived from the area under the binding isotherms according to the equation[27]

$$\pi = 2.303RT \int_{\log[S]_{\bar{\nu}=0}}^{\log[S]_{\bar{\nu}}} \bar{\nu}\, d \log[S] \tag{5}$$

The binding potential is related to the apparent binding constant, K_{app}, as follows:

$$\pi = RT \ln(1 + K_{app}[S]^{\bar{\nu}}) \tag{6}$$

The Gibbs energy of binding is calculated from

$$\Delta G_{\bar{\nu}} = -\frac{RT}{\bar{\nu}} \ln K_{app} \tag{7}$$

On the basis of the high number of previously obtained binding sites where a ligand can be adsorbed, there is a statistical contribution that cannot be neglected, except for the totally free and saturated protein.[28] Thus, the following relation can be considered for the binding of ionic surfactants to proteins:

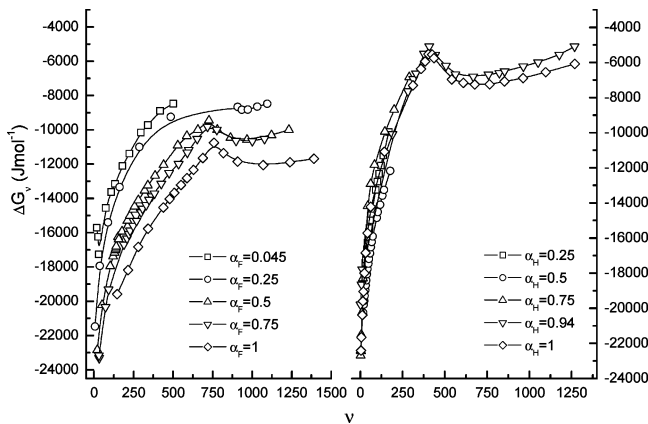$$K_{app} = \Omega_{g_1,g_2,\bar{\nu}} K_{app,int} \tag{8}$$

Figure 4. Gibbs energies of interaction per mol of HSA as a function of the number of sodium perfluorooctanoate (left-hand plots) and sodium octanoate (right-hand plots) molecules bound to the HSA molecule ($\bar{\nu}$).

Figure 5. Gibbs energies of interaction per mol of HSA as a function of the number of sodium perfluorooctanoate (left-hand plots) and sodium dodecanoate (right-hand plots) molecules bound to the HSA molecule ($\bar{\nu}$).

where $K_{app,int}$ and $\Omega_{g_1 g_2, \bar{\nu}}$ are the apparent intrinsic binding constant and the number of arrangements associated with the formation of a complex formed by the protein and $\bar{\nu}$ ligands, respectively. The number of arrangements is given by

$$\Omega_{g_1 g_2, \bar{\nu}} = \frac{g_1!}{(g_1 - \bar{\nu})! \bar{\nu}!} \tag{9}$$

when $\bar{\nu} \leq g_1$ and by

$$\Omega_{g_1 g_2, \bar{\nu}} = \frac{g_2!}{(g_2 - (\bar{\nu} - g_1))!(\bar{\nu} - g_1)!} \tag{10}$$

when $g_1 \leq \bar{\nu} \leq g_2$.

Thus, the Gibbs energy of binding can be written as $\Delta G_{\bar{\nu}} = \Delta G_{stat,\bar{\nu}} + \Delta G_{int,\bar{\nu}}$ where $\Delta G_{stat,\bar{\nu}}$ and $\Delta G_{int,\bar{\nu}}$ are the statistical and intrinsic Gibbs free energy of binding per mole of ligand, respectively, defined as

$$\Delta G_{stat,\bar{\nu}} = -\frac{RT}{\bar{\nu}} \ln \Omega_{g_1, g_2, \bar{\nu}} \tag{11}$$

and

$$\Delta G_{\bar{\nu}} = -\frac{RT}{\bar{\nu}} \ln K_{app,int} \tag{12}$$

Figures 4 and 5 show $\Delta G_{\bar{\nu}}$ as a function of $\bar{\nu}$ for the systems under study. The shape of these curves shows that $\Delta G_{\bar{\nu}}$ is large and negative at low values of $\bar{\nu}$, where binding to the high-energy sites occurs, and gradually decreases as saturation is approached. The breaks in the plots correspond to the saturation of the first binding set, and are due to the large change in the statistical contribution. Some differences can be observed between the system under study, which can help us to gain quantitative understanding of the influence of the interactions between fluorocarbon and hydrocarbons on protein adsorption. In the case of the C8HONa/C8FONa system, the breaks remain practically the same for all α, with values of 411 and 752 for C8HONa and C8FONa, respectively, while for C12HONa/C8FONa, these breaks diminish with α, changing from 752 (α_F = 1) to 620 (α_F = 0.5) and from 746 (α_H = 1) to 570 (α_H = 0.5). For the C8HONa/C8FONa system, the saturation of the first binding set is independent of the presence of the other surfactant; this means that both surfactants have different favorite adsorption sites along the protein. However, for the C12HONa/C8FONa system, both surfactants compete for the
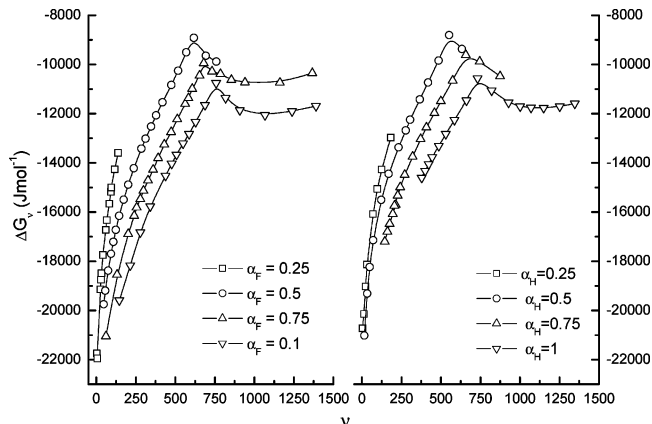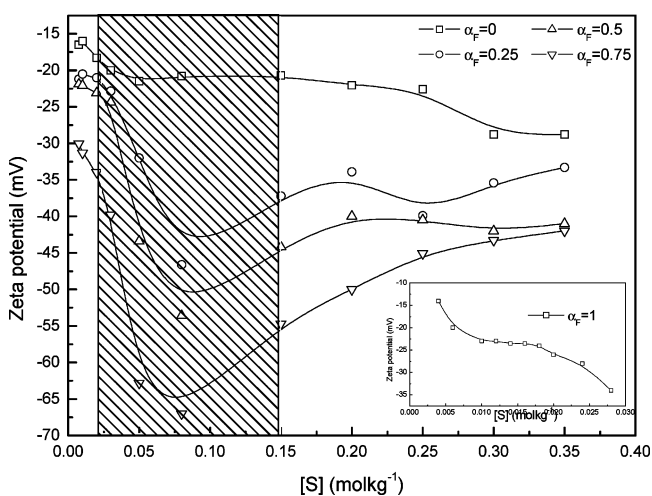

Figure 6. Zeta potential of the HSA−C8HONa/C8FONa system at different mixed (α_F) ratios as a function of the total concentration. The inset shows the zeta potential of the HSA−C8FONa system (α_F = 1).
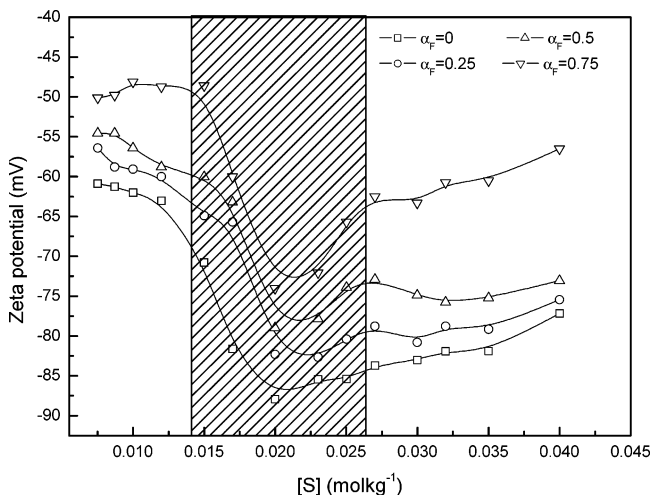

Figure 7. Zeta potential of the HSA−C12HONa/C8FONa system at different mixed (α_F) ratios as a function of the total concentration.

same sites. These facts lead to one idea: the adsorption process (as well as the staked energies) of C8FONa is more closely followed by C12HONa than by C8HONa.

Figures 6 and 7 illustrate the zeta potentials of the HSA−C8HONa/C8FONa and HSA−C12HONa/C8FONa systems,

respectively, at different mixed (α_F) ratios as a function of the total concentration.

The surface charge density enclosed by the shift plane was calculated by means of the following relation for a $z{:}z$ electrolyte[29]

$$\sigma = \frac{\epsilon_r \epsilon_0 k_B T \kappa}{ze}\left[2\sinh\left(\frac{ez\zeta}{2k_B T}\right) + \frac{4}{\kappa a}\tanh\left(\frac{ez\zeta}{4k_B T}\right)\right] \quad (13)$$

where e is the elemental charge, ϵ_0 and ϵ_r are the dielectric constant of vacuum and the relative constant of the solvent, a is the particle radius, and κ is the reciprocal Debye length. The values of the calculated charge vary for each of the systems studied, the lowest values changing from -2.1 to -3.7 μC cm^{-2} (corresponding to the lowest and highest concentrations of the surfactant) for the HSA$-$C8HONa system. On the other hand, the highest values found correspond to the HSA$-$C12HONa system which varies from -8.2 to -11.7 μC cm^{-2} (with maximum values at intermediate concentrations of -12.6 μC cm^{-2}). The net charge density of HSA at pH equal to 7 is -17 μC cm^{-2}, with I, II, and III domains having individual charges of -11, -7, and $+1$ μC cm^{-2}, respectively.[30]

The zeta potential and surface charge density of both quantities exhibit the same pattern in both systems. The zeta potential initially shows a small plateau followed by a sudden decrease and finally an increase at higher concentrations. Given that the net charge of albumin is negative, this increase in the negative charge of the complex is the result of the hydrophobic nature of both surfactants and the presence of hydrophobic cavities in the protein structure.[31] It is worth noting, however, that the initial plateau for the HSA$-$C8HONa/C8FONa system decreases with α_F, a fact correlating with the breaks found for the Gibbs energies of C8FONa. Although those breaks occur at fixed $\bar{\nu}$ (see Figure 4), different concentrations correspond to this value depending on α_F (see Figure 2). Moreover, and following the same line of reasoning, for the C8HONa Gibbs energy break, a value of 0.15 M for [S] has been found. Thus, the intermediate area of the zeta potential plots characterized by the sudden decrease and increase will be limited by the saturation of the first binding set of C8FONa and C8HONa, respectively. A similar conclusion can be extrapolated for the other system under study.

Despite the high degree of correlation between the different plots, one important difference has been found when α_F increases: for the HSA$-$C8HONa/C8FONa system, the zeta potential shifts toward more negative values, while for the HSA$-$C12HONa/C8FONa the shift is toward more positive values. This fact is not surprising considering that the differences in the binding process between the two systems previously described could arise in several protein conformational states.

To gain quantitative understanding of the binding process, the electrical contributions to the Gibbs energies of binding can be estimated from the expression $\pm z_1 e\zeta_i$, where z_i is the charge on the adsorbing ion (here, -1), e is the electronic charge per mole, and ζ_i is the zeta potential.[32] From the zeta-potential values, the electrical contributions of the total Gibbs energies of binding change from 8% at low $\bar{\nu}$ values to 38% at high ones (for the HSA$-$C8HONa/C8FONa system) and from 21% to 67% (for the HSA$-$C12HONa/C8FONa system).

Difference absorption spectra of HSA in the presence of C8HONa/C8FONa and C12HONa/C8FONa are presented in Figures 8 and 9, respectively (spectra corresponding to the other mixed surfactant ratios follow the same pattern). First of all, the lack of isobestic points reveals that only one species is
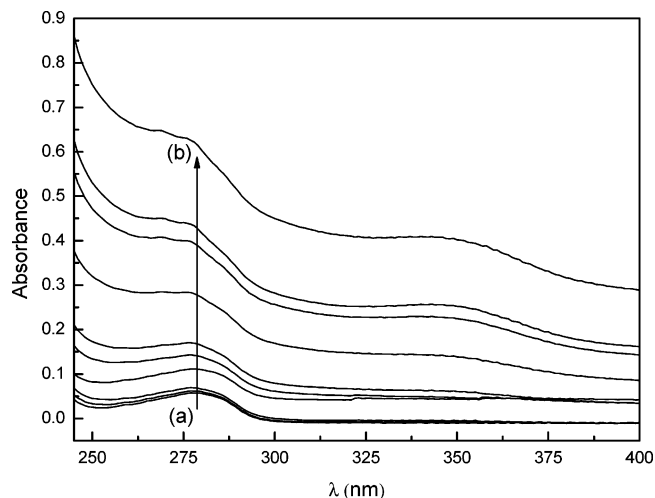

Figure 8. Difference absorption spectra of HSA (0.125% w/v) in the presence of the C8HONa/C8FONa system ($\alpha_F = 0.25$) at different total concentrations from (a) 0.0075 to (b) 0.35 mol kg^{-1}.
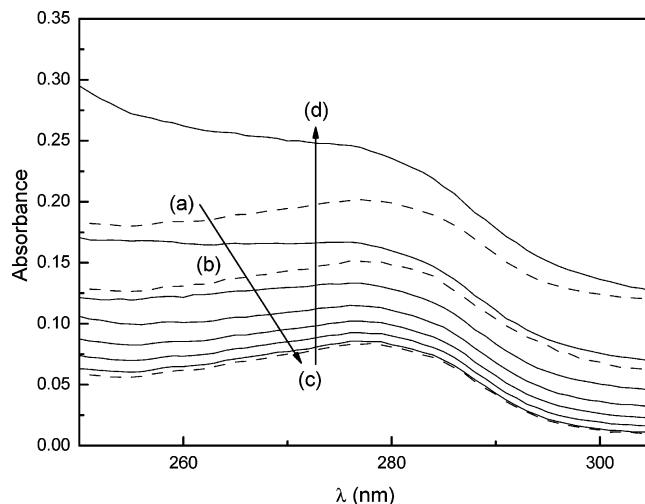

Figure 9. Difference absorption spectra of HSA (0.125% w/v) in the presence of the C12HONa/C8FONa system ($\alpha_F = 0.25$) at different total concentrations: (a) 0.0075, (b) 0.006, and (c) 0.0067 mol kg^{-1} plotted with dash line, and from (c) to (d) 0.03 mol kg^{-1} plotted with solid line.

present in the solution,[33] and if we assume that the surfactants do not contribute to the absorption spectrum (in these systems, in the near-UV, the major factor responsible for the absorbance is tryptophan with a maximum at 280 nm[34]) then we can conclude that the surfactant mixture spreads equally over the total of protein molecules present in solution. Differences in the spectra corresponding to both systems under study are basically limited to the existence of a peak (just at higher concentrations) of the HSA$-$C8HONa/C8FONa system, at 345 nm. On the other hand, we have not found red shifts in the spectra at any concentration for our systems. In previous studies it has been found that the binding of octanoate or dodecanoate results in red shifts of the protein spectra because of the perturbation of tyrosine and phenylalanine.[35] The lack of shifts in our plots could therefore be explained by assuming a tryptophan blue shift due to its interaction with perfluoro-octanoate.

Figures 10 and 11 show the absorbance changes for the systems under study for the 280 nm difference spectra band as a function of total concentration. The plots show that while for the HSA$-$C8HONa/C8FONa system there is a gradual change
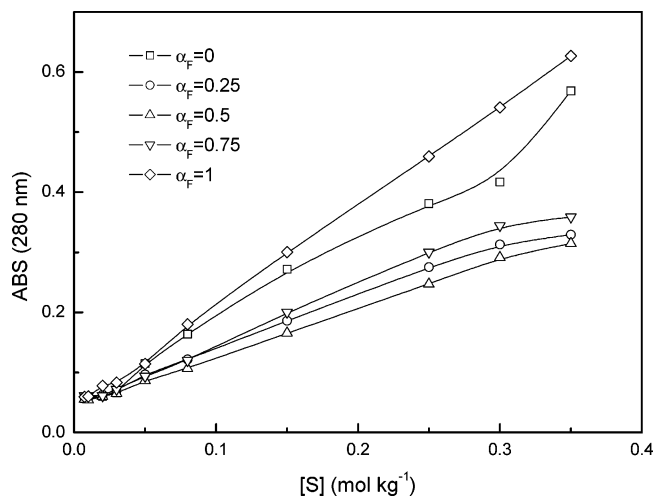
Figure 10. Absorbance of HSA in the presence of C8HONa/C8FONa at different mixed ratios.
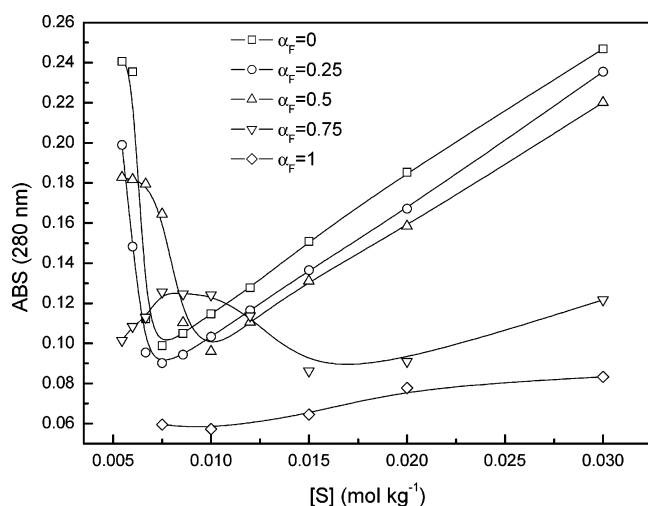

Figure 11. Absorbance of HSA in the presence of C12HONa/C8FONa at different mixed ratios.

in the absorbance, for the HSA−C12HONa/C8FONa system there is a transition region over which the absorbance undergoes significant change with concentration. It is well-know that proteins undergo changes in their natural state by the action of surfactants.[27] Thus, the data suggest that, upon interaction with both systems, HSA undergoes a more significant change in conformation with C12HONa/C8FONa.

4. Conclusions

The complex formation between HSA and sodium perfluorooctanoate/sodium octanoate and sodium perfluorooctanoate/sodium dodecanoate systems at different mixed ratios has been studied using different experimental techniques and theoretical models. The results obtained are summarized as follows. As a first step, we have studied the solution properties of the surfactant mixtures in the absence of protein, concluding that the C12HONa/C8FONa system forms mixed micelles with repulsive interactions while the C8HONa/C8FONa system does not form mixed micelles.

The binding isotherms were subsequently constructed. From these plots we observed how the cooperative binding is higher for the C12HONa/C8FONa system which is the only system able to form mixed micelles. The number of molecules adsorbed onto the protein is similar for C8FONa and C12HONa which have similar cmc and solution properties. Thus, it could be that

hydrocarbon surfactants with a hydrocarbon chain 1.5 times longer than the corresponding fluorocarbon have similar patterns in the presence of globular proteins.

Two binding sets have been proposed for the two systems under study. However, taking into account the binding isotherms and the Gibbs energy of binding, we have found that for the C8HONa/C8FONa system, the saturation of the first binding set is independent of the presence of the other surfactant, whereas for the C12HONa/C8FONa system, both surfactants compete for the same adsorption sites onto the protein.

Zeta-potential measurements show a transition area for both systems whose limits are very close to the break points obtained from Gibbs energies of binding. However, when the C8FONa ratio in the mixture is increased, the zeta potential of the HSA−C8HONa/C8FONa system shifts toward more negative values, while for the HSA−C12HONa/C8FONa system, the shift is toward more positive values. This fact could be related to different protein conformational states. Thus, changes in protein conformation, such as unfolding, very often lead to large changes in the UV−vis emission. The absorbance of the HSA−C8HONa/C8FONa system exhibits an increase of the total concentration, but for the HSA−C12HONa/C8FONa system there is a steep initial decrease followed by an increase. In the first case, the absorption spectra indicate that the unfolding process of HSA involves only a native and unfolded state; that is, the reaction follows a two-state process. However, in the second case, the plots point out that at least one relatively stable intermediate was formed during the unfolding of HSA.

Finally, we would like to point out that the picture of the mixed fluorocarbon/hydrocarbon/HSA system reported here could provide a key that paves the way for future biochemical and biomedical applications, for example, in the recovery of proteins and in the formation of protein based gel.[36]

References and Notes

(1) Ananathapadmanabhan, K. P. *Interaction of Surfactants with Polymers and Proteins*; CRC Press: Boca Raton, FL, 1993.
(2) Sun, M. L.; Tilton, R. D. *Colloids Surf., B* **2001**, *20*, 281.
(3) Shinoda, K.; Nomura, T. *J. Phys. Chem.* **1980**, *84*, 365.
(4) Funasaki, N. *Mixed Surfactant Systems*; Marcel Dekker: New York, 1993.
(5) Ruso, J. M.; Taboada, P.; Martinez-Landeira, P.; Prieto, G.; Sarmiento, F. *J. Phys. Chem. B* **2001**, *105*, 2644.
(6) Messina, P.; Prieto, G.; Dodero, V.; Ruso, J. M.; Schulz, P. C.; Sarmiento, F. *Biopolymers* **2005**, *79*, 300.
(7) Messina, P.; Prieto, G.; Ruso, J. M.; Sarmiento F. *J. Phys. Chem. B* **2005**, *109*, 15566.
(8) Blanco, E.; González-Pérez, A.; Ruso, J. M.; Pedrido, R.; Prieto, G.; F. Sarmiento, F. *J. Colloid Interface Sci.* **2005**, *288*, 247.
(9) Lu, J. R.; Su, T. J.; Penfold, J. *Langmuir* **1999**, *15*, 6975.
(10) Kissa, E. *Fluorinated Surfactants: Synthesis, Properties, Applications*; Marcel Dekker: New York, 1994.
(11) Carter, D. C.; Ho, J. X. *Adv. Protein Chem.* **1994**, *45*, 153.
(12) Shedlovsky, T. *J. Am. Chem. Soc.* **1932**, *54*, 1411.
(13) Chambers, J. F.; Stokes, J. M.; Stokes, R. H. *J. Phys. Chem.* **1956**, *60*, 985.
(14) Hidalgo-Alvarez, R. *Adv. Colloid Interface Sci.* **1991**, *34*, 217.
(15) Shinoda, K.; Kobasashi, M.; Yamaguchi, N. *J. Phys. Chem.* **1987**, *91*, 5292.
(16) De Lisi, R.; Inglese, A.; Milioto, S.; Pellerito A. *Langmuir* **1997**, *13*, 192.
(17) Stimson, M. F. *Am. J. Phys.* **1955**, *23*, 614.
(18) Clint, J. H. *J. Chem. Soc., Faraday Trans. 1* **1975**, *71*, 1327.

(19) Rubingh, D. N. *Solution Chemistry of Surfactants*; Plenum Press: New York, 1979.

(20) Hoffmann, H.; Pössnecker, G. *Langmuir* **1994**, *10*, 381.

(21) (a) Moya, S. E.; Schulz, P. C. *Colloid Polym. Sci.* **1999**, *277*, 735. (b) Schulz, P. C.; Minardi, R. M.; Ruano, B. *Colloid Polym. Sci.* **1999**, *277*, 837. (c) Mukerjee, P.; Yang, A. Y. S. *J. Phys. Chem.* **1976**, *89*, 1388.

(22) Miyagishi, J. H.; Ishibai, Y.; Asakawa, T.; Nishida, M. *J. Colloid Interface Sci.* **1985**, *103*, 164.

(23) Benrraou, M.; Baley, B.; Zana. R. *J. Colloid Interface Sci.* **2003**, *267*, 519.

(24) He, X. M.; Carter, D. C. *Nature* **1992**, *358*, 209.

(25) Bordbar, A. K.; Saadati, Z.; Sohrabi, N. *Acta Biochim. Pol.* **2004**, *51*, 963.

(26) Rafati, A. A.; Bordbar, A. K.; Gharibi, H.; Amino, M. K.; Safarpour, M. A. *Bull. Chem. Soc. Jpn.* **2004**, *77*, 1111.

(27) Jones, M. N.; Chapman, D. *Micelles*, *Monolayers and Biomembranes*; Wiley-Liss: New York, 1995.

(28) Bordbar, A. K.; Saboury, A. A.; Housaindokht, M. R.; Moosavi-Movahedi, A. A. *J. Colloid Interface Sci.* **1997**, *192*, 415.

(29) Quesada-Perez, M.; Callejas-Fernández, J.; Hidalgo-Alvarez, R. *Colloid Surf. A* **1999**, *159*, 239.

(30) Peters, T. J. *All About Albumin: Biochemistry*, *Genetics and Medical Applications*; Academic Press: San Diego, CA, 1996.

(31) Kragh-Hansen, U. *Pharmacol. Rev.* **1981**, *33*, 17.

(32) Hunter, R. J. *Zeta Potential in Colloid Science*; Academic Press: London, 1981.

(33) Connors, K. A. *Binding Constants: The Measurements of Molecular Complex Stability*; Wiley: New York, 1987.

(34) Lakowicz, J. R. *Principles of Fluorescence Spectroscopy*; Kluwer Academic/Plenum Publishers: New York, 1999.

(35) Polet, H.; Steinhardt, J. *Biochemistry* **1968**, *7*, 1348.

(36) Sesta, B.; Gente, G.; Ioviono, A.; Laureti, F.; Michiotti, P.; Paiusco, O.; Palacios, A. C.; Persi, L.; Princi, A.; Sallustio, S.; Sarnthein-Graf, C.; Capalbi, A.; La Mesa, C. *J. Phys. Chem. B* **2004**, *108*, 3036.